Available online at www.sciencedirect.com

SciVerse ScienceDirect

Ceramics International 38 (2012) 5629–5636

CERAMICS INTERNATIONAL

www.elsevier.com/locate/ceramint

Structure and luminescence properties of Eu^{3+} doped TiO_2 nanocrystals and prolate nanospheroids synthesized by the hydrothermal processing

M. Vranješ [a], J. Kuljanin-Jakovljević [a], T. Radetić [b], M. Stoiljković [a], M. Mitrić [a], Z.V. Šaponjić [a,*], J. Nedeljković [a]

[a] Vinča Institute of Nuclear Sciences, University of Belgrade, P.O. Box 522, 11001 Belgrade, Serbia
[b] Faculty of Technology and Metallurgy, University of Belgrade, Karnegijeva 4, 11120 Belgrade, Serbia

Received 6 February 2012; received in revised form 2 April 2012; accepted 2 April 2012
Available online 12 April 2012

Abstract

We report on a new approach to the synthesis of Eu^{3+} doped TiO_2 nanocrystals and prolate nanospheroids. They were synthesized by shape transformation of hydrothermally treated titania nanotubes at different pH and in the presence of Eu^{3+} ions. The use of nanotubes as a precursor to the synthesis of Eu^{3+} doped TiO_2 nanocrystals and prolate nanospheroids opens the possibility of overcoming the problems related to molecular precursors. The shapes and sizes of the nanotubes, Eu^{3+} doped TiO_2 nanocrystals and prolate nanospheroids were characterized by transmission electron microscopy (TEM) technique. Crystal structures of the resultant powders were investigated by X-ray diffraction (XRD) analysis. The percentage ratio of Eu^{3+} to Ti^{4+} ions in doped nanocrystals was determined using inductively coupled plasma atomic emission spectroscopy. The optical characterization was done by using fluorescence and ultraviolet-visible reflection spectroscopies. An average size of faceted Eu^{3+} doped TiO_2 nanocrystals was 13 nm. The lateral dimensions of Eu^{3+} doped TiO_2 prolate nanospheroids varied from 14 to 20 nm, while the length varied from 40 to 80 nm, depending on precursor concentrations. The XRD patterns revealed the homogeneous anatase crystal phase of Eu^{3+} doped TiO_2 nanocrystals and prolate nanospheroids independently of the amount of dopant. A postsynthetic treatment (filtration or dialysis) was applied on the dispersions of the doped nanoparticles in order to study the influence of the dopant position on photoluminescence (PL) spectra. In the red spectral region, room temperature PL signals associated with $^5D_0 \rightarrow {}^7F_J$ ($J = 1$–4) transitions of Eu^{3+} were observed in all samples. The increased contribution of dopants from the interior region of dialyzed nanocrystals to photoluminescence was confirmed by the increase of R value.

Keywords: B. spectroscopy; B. X-ray methods; C. optical properties; D. TiO_2; Hydrothermal synthesis

1. Introduction

Rare earth cation doped materials [1–4] are attracting huge interest in the scientific community and industry due to their potential in a wide range of applications [5]. In particular, doping semiconductors with rare earth ions opens the possibility of controlling the optical properties by the band gap structure of the semiconductor host [6,7].

Titanium dioxide (TiO_2) in the anatase crystal form has a wide band gap (3.2 eV) and high transparency, i.e. low absorbance in the visible ($\lambda_{abs} < 390$ nm) and infrared wavelength region. Such properties make TiO_2 a promising host material for dopant ions. Also, relatively high refractive index, good chemical, thermal and mechanical properties of TiO_2 make it useful for optical devices [6,8]. For example, red emitting phosphors based on Eu^{3+} doped TiO_2 fulfilled conditions for white LED applications [9].

Until now, a large number of synthetic procedures have been reported for the preparation of rare-earth-doped nanoparticles. Most of them are based on wet chemical methods such as: sol–gel, hydrothermal processing and inverse micelle techniques using molecular precursors [8,10]. The difference in radius between the dopant and host ions can lead to ''self-purification'' of the dopant ions from the host lattice independently of the crystalline state, imposing serious limitations on application of those methods. In order to eliminate the problem of ''self-purification'', we used nanotubes instead of molecular precursors. An increase of activation energy for nucleation of

* Corresponding author. Tel.: +381 11 3408193; fax: +381 11 3408607.
E-mail address: saponjic@vinca.rs (Z.V. Šaponjić).

0272-8842/$36.00
http://dx.doi.org/10.1016/j.ceramint.2012.04.004

nanocrystals, which leads to exclusion of dopant ions from nanoparticles during the growth phase from molecular precursors, could be avoided when using nanotubes as precursors.

In this study we report on the synthesis and characterization of Eu^{3+} doped TiO_2 faceted nanocrystals and prolate nanospheroids. The Eu^{3+} doped TiO_2 faceted nanocrystals and prolate nanospheroids were synthesized by shape transformation of titania nanotubes as precursors in the presence of Eu^{3+} ions during hydrothermal treatment. Morphology of the faceted nanocrystals and prolate nanospheroids was characterized by transmission electron microscopy (TEM). The crystal structure was determined by X-ray diffraction (XRD) analysis. Room temperature PL spectra were measured by direct excitation of dopant ions (λ_{exc} = 396 nm).

2. Experimental methods

Titania nanotubes were synthesized according to the procedure described elsewhere [11]. The same concentration (6.4×10^{-4} M) of Eu^{3+} ions was used in the precursor dispersions for the synthesis of doped TiO_2 faceted nanocrystals and prolate nanospheroids.

Eu^{3+} doped TiO_2 faceted nanocrystals were synthesized applying hydrothermal treatment (90 min/250 °C, Teflon vessel – Parr acid digestion bomb) of dispersion of 3×10^{-2} M (25 mg/10 mL) titania nanotubes (pH 3) in the presence of 6.4×10^{-4} M $Eu(NO_3)_3$. Prior to the hydrothermal treatment, the suspension was stirred at room temperature for 3 h. In order to remove excess Eu^{3+} ions, the dispersions of Eu^{3+} doped TiO_2 faceted nanocrystals were filtrated or dialyzed against acidified water (pH 3) at 4 °C for three days. The water was changed daily.

The hydrothermal processing (90 min/250 °C) of scrolled titania nanotube dispersions (pH ~5–6) in various concentrations (25 mg/10 mL, 50 mg/10 mL, 75 mg/10 mL) and in the presence of 6.4×10^{-4} M $Eu(NO_3)_3$ was used for the synthesis of Eu^{3+} doped TiO_2 prolate nanospheroids. Postsynthetic treatments of the doped prolate nanospheroids (by filtration or dialysis against water for three days at 4 °C) were applied with the aim of removing excess dopant ions from the surface.

Morphology (size and shape) of titania nanotubes, Eu^{3+} doped TiO_2 faceted nanocrystals and prolate nanospheroids was studied by TEM technique. Characterization of the titania nanotubes was performed in a Hitachi H-700 FA TEM at 125 kV, while a JEOL 100CX operating at 100 kV was used to characterize the doped faceted nanocrystals and prolate nanospheroids.

The X-ray diffraction (XRD) measurements were carried out in a BRUKER D8 ADVANCE diffractometer in theta/theta reflection geometry with parallel beam optics achieved by multilayer Göbel mirror. Diffraction data for the structure analysis were collected in 2θ range from 10° to 80°, with steps of 0.05° and 10 s counting time per step.

The percentage ratio of Eu^{3+} ions to Ti^{4+} ions in doped nanocrystals and prolate nanospheroids was determined using inductively coupled plasma (ICP) atomic emission spectroscopy: ICAP 6000 series (Thermo Electron Corporation). Prior to the ICP measurements, powdered specimens were dispersed in 10 mL of concentrated sulfuric acid and hydrothermally treated for 60 min at 250 °C in a Teflon vessel (Parr acid digestion bomb). The concentration of Eu^{3+} ions in the filtrated specimen of TiO_2 faceted nanocrystals was 0.7 at.% of the amount of Ti^{4+} ions, while the concentration of Eu^{3+} ions in the dialyzed sample of TiO_2 faceted nanocrystals was 0.24 at.%. The concentrations of Eu^{3+} in the filtrated prolate nanospheroids were 0.5, 0.34 and 0.2 at.% of the amount of Ti^{4+} ions, in the samples with 25, 50 and 75 mg/10 mL of the starting concentrations of titania nanotubes, respectively.

The photoluminescence (PL) spectra of powdered samples were recorded at room temperature on a Perkin-Elmer LS-45 Fluorescence Spectrometer, in front-face mode (λ_{exc} = 396 nm) and with a time delay of 0.04 ms.

Reflection spectrum of Eu^{3+}:TiO_2 powder was recorded at room temperature using Thermo Scientific Evolution 600 UV/Vis spectrophotometer.

3. Results and discussions

Precursor dispersion of titania nanotubes was synthesized by hydrothermal processing of commercial TiO_2 powder in proton deficient aqueous solution [11]. Conventional TEM image of the nanotubes is shown in Fig. 1. Uniform size distribution of nanotube diameters ($d \sim 10$ nm) was observed. The length of the nanotubes was in a wide range from one hundred to a few hundred nanometers. The nanotubes had an open-ended multiwall structure. Crystal structure of the nanotubes was defined as a quasianatase: axially symmetric, with distorted octahedral coordination and a large portion of undercoordinated sites on the surface [12].

Our previous work has shown that such nanotubular material is a good candidate for the synthesis of doped TiO_2 nanocrystals through reshaping and structural reorganization [13,14]. By using the titania nanotubes as the precursor for the synthesis of Eu^{3+} doped TiO_2 nanocrystals and prolate nanospheroids, the problem related to the nucleation stage of nanocrystals was avoided.

Prior to the hydrothermal treatment, the dispersion of the titania nanotubes and $Eu(NO_3)_3$ was mixed for 3 h. During that

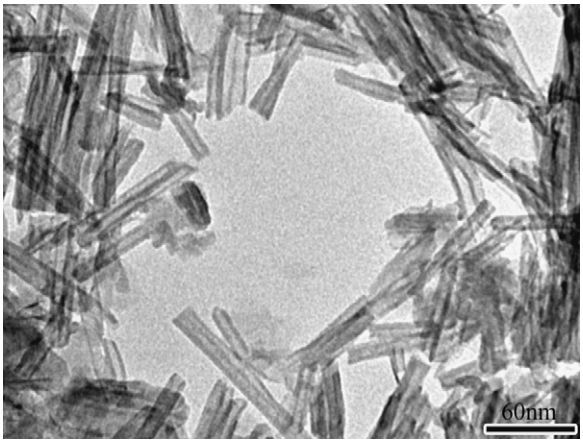

Fig. 1. Bright field TEM image of titania nanotubes.

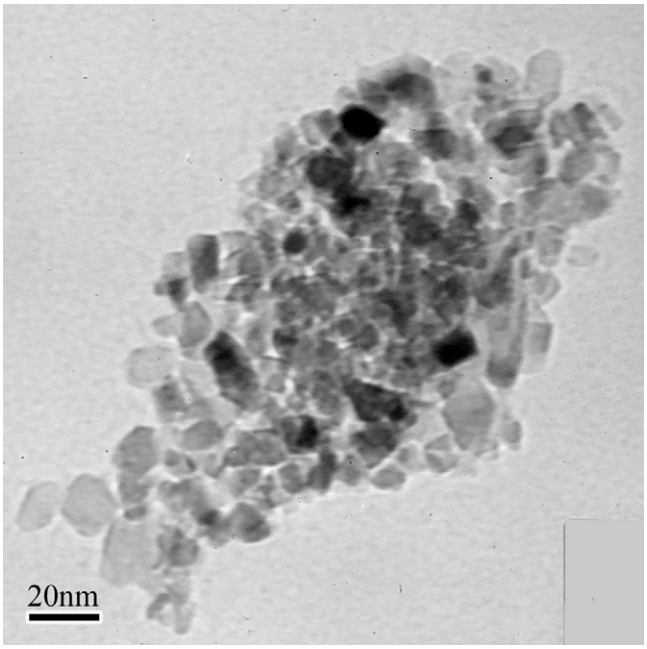

Fig. 2. Bright field TEM image of 0.24 at.% Eu^{3+} doped TiO_2 nanocrystals.

phase of the synthesis, it was possible for Eu^{3+} ions to enter the interlayer space or the inner surface of the walls of nanotubes, since the radius of Eu^{3+} ion (0.0947 nm in octahedral coordination) [6,15] is much smaller than the interwall distance in the nanotube (0.73 nm) [12]. Also, Eu^{3+} ions can be adsorbed at the undercoordinated defect sites existing on the surface of the titania nanotubes [13]. These undercoordinated defect sites are pentacoordinated highly reactive interior or exterior Ti atoms (∼40%) [12]. Hydrothermal treatment of the nanotubes dispersion (concentration 25 mg/10 mL, pH 3) containing Eu^{3+} ions (6.4×10^{-4} M) resulted in the formation of faceted Eu^{3+} doped TiO_2 nanocrystals. Faceted nanocrystals with an average dimension of 13 nm are shown in Fig. 2.

The hydrothermal treatment of nanotubes dispersion in the presence of Eu^{3+} ions at higher pH (pH 5–6) resulted in the formation of Eu^{3+} doped TiO_2 prolate nanospheroids, Fig. 3. TEM characterization showed that the average dimension of synthesized Eu^{3+} doped TiO_2 prolate nanospheroids depends on the concentration of titania nanotubes and concentration of Eu^{3+} ions in precursor dispersion. The smallest amount of titania nanotubes (25 mg/10 mL) in the precursor dispersion containing Eu^{3+} used for the hydrothermal synthesis of the nanospheroids resulted in the nanocrystals with an average length of 40–50 nm, while the lateral dimension was in the 14–16 nm range, Fig. 3a. Increasing the concentration of nanotubes in precursor dispersion to 50 mg/10 mL did not cause major changes in the dimensions of Eu^{3+} doped TiO_2 prolate nanospheroids (not shown). A further increase in the concentration of nanotubes in precursor dispersion (75 mg/10 mL) resulted in a wider particle size distribution and in increased average dimensions of Eu^{3+} doped TiO_2 prolate nanospheroids. The lateral dimension was in the range 15–20 nm, while the length was in the 50–80 nm range, Fig. 3b.

Larger dimensions of the prolate nanospheroids obtained, when the concentration of the nanotubes in precursor dispersion was highest (75 mg/10 mL), are in agreement with lower concentration of Eu atoms presented in this system. In other

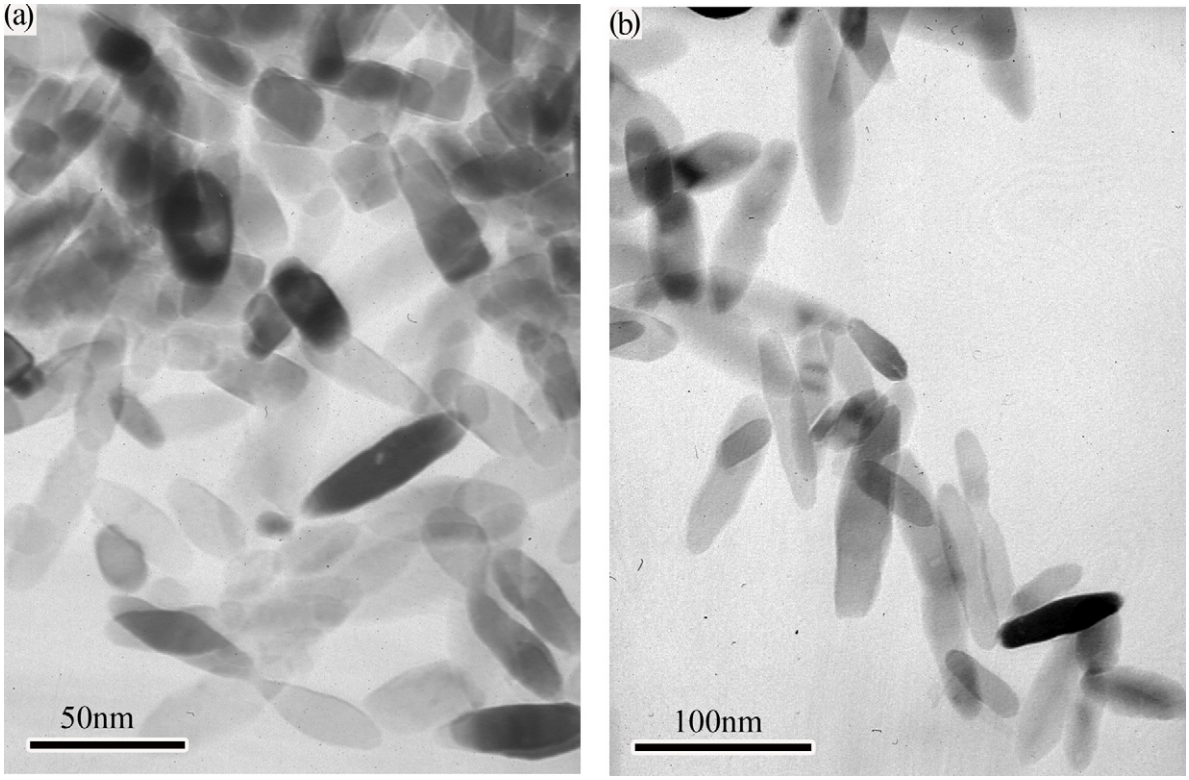

Fig. 3. Bright field TEM images of Eu^{3+} doped TiO_2 prolate nanospheroids with different dopant concentrations: 0.42 at.% (a) and 0.041 at.% (b).

words, an increase in the dopant concentration in prolate nanospheroids causes the decrease of their size. It is well known that the presence of Eu atoms decreases the crystallite size of Eu^{3+} doped TiO_2 nanocrystals because the growth of TiO_2 crystallites is hindered by the formation of Eu–O–Ti bonds on the crystallite surface or in interstices of TiO_2 nanocrystals [16,17].

The powder X-ray diffraction analysis of Eu^{3+} doped TiO_2 nanocrystals and nanospheroids showed the existence of a homogeneous anatase (tetragonal, JCPDS 84-1286) crystal phase, Fig. 4. The presence of all the characteristic anatase diffraction peaks with preserved intensity ratios shows random orientation of the TiO_2 nanoparticles, Fig. 4. The formation of the rutile crystalline phase was not induced by applied synthetic procedure as no characteristic peaks corresponding to the rutile phase were detected. Although the anatase crystal structure, according to XRD data, appears undisturbed after incorporation of Eu^{3+} ions either substitutionally or interstitially, there is still the possibility of local distortions.

It is known that the solubility of Eu^{3+} ions within the anatase lattice is limited due to a big difference in size between ionic radii of Ti^{4+} (0.074 nm) and Eu^{3+} (0.0947 nm) in octahedral coordination [18]. According to Li et al. [6], the maximum value of Eu^{3+} ions that can be successfully doped into a TiO_2 lattice is 0.5 at.%, above which $Eu_2Ti_2O_7$ pyrochlor can be formed as a final product. XRD data, Fig. 4, did not show inhomogeneity caused by the formation of Eu_2O_3 or $Eu_2Ti_2O_7$ aggregates. Further, both $Eu_2Ti_2O_7$ and Eu_2O_3 are able to exhibit emission that is actually different from those of Eu^{3+} doped TiO_2 nanocrystals due to different local environments of Eu^{3+} ions, tetragonal versus cubic [6].

There is a negligible modification in reflection properties of 0.24 at.% Eu^{3+} doped TiO_2 nanocrystals with respect to reflection properties of undoped TiO_2 nanocrystals synthesized in the same way, as it can be seen from the reflection spectra in Fig. 5. Such dopant amount did not significantly affect the onset of absorption calculated from the plot of $F(R_\infty)^2$ versus photon energy, inset in Fig. 5, and consequently the band gap value of doped TiO_2 nanocrystals remains almost unchanged [19,20]. Similarly, even the highest concentrations of Eu^{3+} ions doped in the TiO_2 prolate nanospheroids (0.42 at.%) did not significantly affect the reflection spectra. Consequently, the band gap of TiO_2 was not affected by the presence of the Eu^{3+} ions. In addition, the white color of the samples indicated that, independently of the shape, the Eu^{3+}/TiO_2 nanocrystals and prolate nanospheroids did not have too many oxygen vacancies [21].

In general, Eu^{3+} dopant ions can occupy at least two different sites with different binding energies in titania nanocrystals: core octahedral sites (less likely to be occupied due to radius difference between Eu^{3+} and Ti^{4+}) and undercoordinated surface sites, in addition to physisorption on the particle surface [13,22] and interstitial incorporation. In order to investigate the influence of the position of dopant on photoluminescence spectra, the postsynthetic treatment (filtration or dialysis) was applied to the dispersions of the doped nanocrystals and prolate nanospheroids.

The concentration of Eu^{3+} ions in the samples of doped TiO_2 prolate nanospheroids decreased as the amount of nanotubes in precursor solutions increased. Percentage ratios of Eu^{3+} ions to Ti^{4+} ions in the filtrated doped TiO_2 nanospheroids were 0.5, 0.34, and 0.2 at.% in the samples with 25, 50 and 75 mg/10 mL of nanotubes in precursor solutions, respectively. On the other hand, the application of dialysis to the suspension of Eu^{3+} doped TiO_2 prolate nanospheroids resulted in the decrease of the dopant percentage within all samples. Percentage ratios of Eu^{3+} ions to Ti^{4+} ions in dialyzed nanospheroids were 0.42, 0.18, and 0.041 at.% in the samples with 25, 50 and 75 mg of nanotubes in precursor solutions, respectively. A discrepancy between the concentration of dopant ions in the dialyzed samples of TiO_2 doped nanocrystals (0.24 at.%) and the prolate nanospheroids (0.42 at.%) when the amounts of nanotubes in precursor solutions were the same (25 mg/10 mL) should be noted. This is an indication of different amounts of Eu^{3+} ions doped in the undercoordinated surface defect sites and on the surfaces of TiO_2 nanocrystals and prolate nanospheroids. Owing to the larger amount of undercoordinated surface defect sites in the nanocrystals compared with the nanospheroids and higher total surface area, a smaller amount of doped Eu^{3+} ions in TiO_2 nanocrystals (0.24 at.%) is expected after dialysis [13,23].

Due to the charge imbalance and a big mismatch in ionic radii between the dopant ion and Ti^{4+}, besides the existence of multiple sites for incorporation of Eu^{3+} ions into the anatase TiO_2 nanocrystals and prolate nanospheroids, it is reasonable to

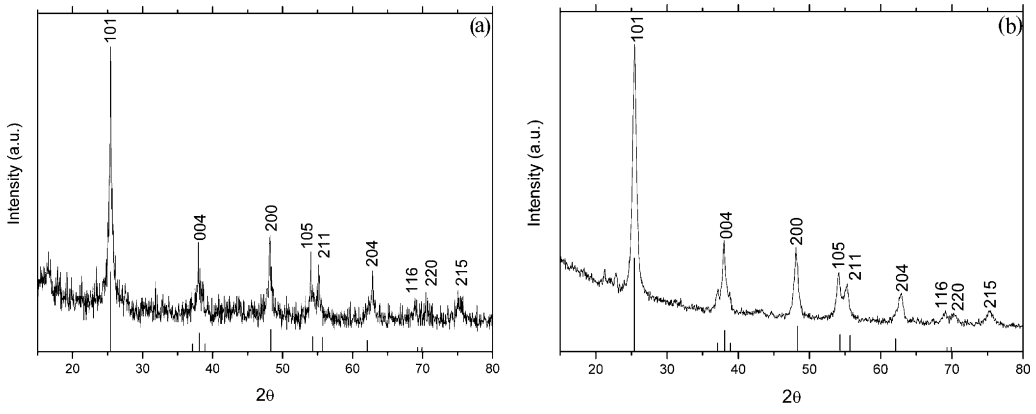

Fig. 4. XRD spectra of 0.24 at.% Eu^{3+} doped TiO_2 nanocrystals (a) and 0.42 at.% Eu^{3+} doped TiO_2 prolate nanospheroids (b).

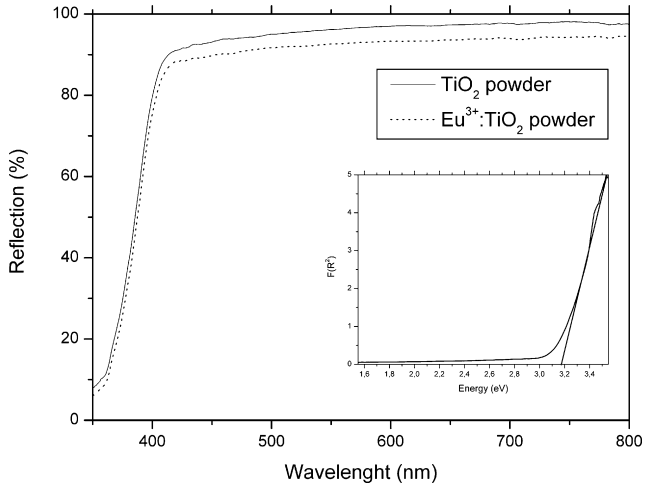

Fig. 5. Reflection spectra of 0.24 at.% Eu^{3+} doped TiO_2 nanocrystals and bare TiO_2 nanocrystals.

expect some lattice defects/distortions in the TiO_2 crystal structure, as it has been observed for the titanate doped with other rare earth ions [24]. The difference between the chemical properties of the host ions and the dopant rare earth ions could lead to sequential precipitation of the dopant ions if they are used in higher concentration; as a result they can be simply absorbed on a nanoparticle surface. In the case when the nanoparticle surface is covered with hydroxyl groups, which is the characteristic of TiO_2 nanocrystals, the probability of nonradiative relaxations of rare earth ions increases [25].

The emission spectrum of Eu^{3+} cations consists of the bands mainly located in the red spectral region between 590 and 750 nm, corresponding to the transition from the excited $^5D_0$ electronic state to the split ^7F_J ($J = 0$–4) sublevels of its $4f^6$ configuration [26]. The energy levels of the Eu^{3+} ion are not affected by different hosts, due to the shielding effect of the $4f$ electrons of Eu^{3+} ion by outer shell $5s$ and $5p$ electrons. The energy level splitting into up to $2J + 1$ sublevels is the consequence of the local crystal field surrounding the Eu^{3+} ion [2].

Emission spectra of the filtrated (0.7 at.% Eu^{3+}) and dialyzed (0.24 at.% Eu^{3+}) samples of Eu^{3+} doped TiO_2 nanocrystals are shown in Fig. 6a. Photoluminescence (PL) measurements have shown that the Eu^{3+} doped TiO_2 nanocrystals exhibit four characteristic $^5D_0$ emissions of Eu^{3+}. The emissions were centered at 594, 617, 653 and 700 nm and were assigned to the $^5D_0 \rightarrow {}^7F_1$, $^5D_0 \rightarrow {}^7F_2$, $^5D_0 \rightarrow {}^7F_3$ and $^5D_0 \rightarrow {}^7F_4$ transitions, respectively.

It is evident that the peak intensities at 594, 617 and 700 nm in PL spectrum of the dialyzed sample are lower than those in the PL spectrum of the filtrated sample. However, the intensity of the emission assigned to the $^5D_0 \rightarrow {}^7F_3$ transition ($\lambda = 653$ nm) is negligibly changed after the dialysis. The overall decrease of PL intensity of the dialyzed sample is a consequence of the removal of the excess Eu^{3+} ions simply adsorbed on the particle surface, as well as Eu^{3+} ions that substitute Ti^{4+} in the undercoordinated defect sites. The existence of the undercoordinated (five coordinated) surface defect sites is inherent to the TiO_2 nanoparticles with a diameter less than 20 nm [27,28]. Such reconstruction of the surface of TiO_2 nanoparticles due to accommodation for high curvature induces changes in the coordination of surface Ti atoms from octahedral (D_{2d}) to square pyramidal structures (C_{4v}) [12,14,27,28]. Dopants in these undercoordinated defect sites may possess C_{4v} site symmetry (square pyramidal structure). Due to the weak binding of dopants in those sites, small particle dimensions and diffusion length, dopant ions can be easily removed applying postsynthetic dialysis treatment of the doped nanoparticles [13].

The peak of the highest intensity in both spectra (Fig. 6a) corresponds to electrically allowed $^5D_0 \rightarrow {}^7F_2$ transition, which has electric-dipole nature. This transition is hypersensitive to the surroundings of the Eu^{3+} ion; it is only allowed for Eu^{3+} ions in the low symmetry sites with no inversion center [29]. Reduction of the peak intensity occurring almost twice in the case of dialyzed Eu^{3+} doped TiO_2 nanocrystals is an indication of a partial elimination of the Eu^{3+} ions from the low symmetry sites. This is in agreement with our previous finding about the higher efficiency of postsynthetic purification of doped samples by dialysis over filtration [13]. However, Eu atoms (as all other dopants) that substitute Ti atoms with the octahedral coordination in the core of TiO_2 nanocrystals are strongly bound to the anatase lattice and cannot be leached out by dialysis.

Magnetically allowed $^5D_0 \rightarrow {}^7F_1$ transition ($\lambda = 594$ nm) which has magnetic-dipole nature is not affected by the surroundings of Eu^{3+} ions [22]. Its intensity is lower than the intensity of electrically allowed transition ($\lambda = 617$ nm) in PL spectra of both the filtrated and dialyzed samples.

Emission spectra of the filtrated and dialyzed samples of Eu^{3+} doped TiO_2 prolate nanospheroids are shown in Figs. 6b–d. In the prolate nanospheroids, as in the case of the doped nanocrystals, the hypersensitive transition $^5D_0 \rightarrow {}^7F_2$, characterized by a peak at $\lambda = 617$ nm, is much stronger compared with other transitions. Such observations lead to the conclusion that in the filtrated and dialyzed samples of Eu^{3+} doped TiO_2 prolate nanospheroids and nanocrystals, Eu^{3+} ions positioned in low symmetry sites prevail. It should be pointed out that the intrinsic site symmetry for Ti^{4+} in the tetragonal anatase crystal lattice is D_{2d}. Substitution of Ti^{4+} ions with larger Eu^{3+} ions leads to the descent of D_{2d} symmetry to a lower site symmetry (S_4, C_{2v}, or D_2) [30,31]. The creation of point defects such as oxygen vacancies (for charge compensation) during the substitution of Ti^{4+} with subvalent Eu^{3+} ions is followed by distortions of TiO_2 lattices and by increased asymmetry.

Emission spectra of the prolate nanospheroids, synthesized using precursor dispersion of nanotubes in a concentration of 25 mg/10 mL, are shown in Fig. 6b. Compared with the filtrated sample (0.5 at.% Eu^{3+}), the decrease of the PL intensity of $^5D_0 \rightarrow {}^7F_2$ transition in the dialyzed sample (0.42 at.% Eu^{3+}) is smaller than in the doped nanocrystals (Fig. 6a). This observation could be an indication of the initially smaller amount of Eu^{3+} ions positioned in the undercoordinated surface defect sites of TiO_2 characterized with (C_{4v}) symmetry which can be affected by dialysis [13]. In general, the amount of undercoordinated surface defect sites in

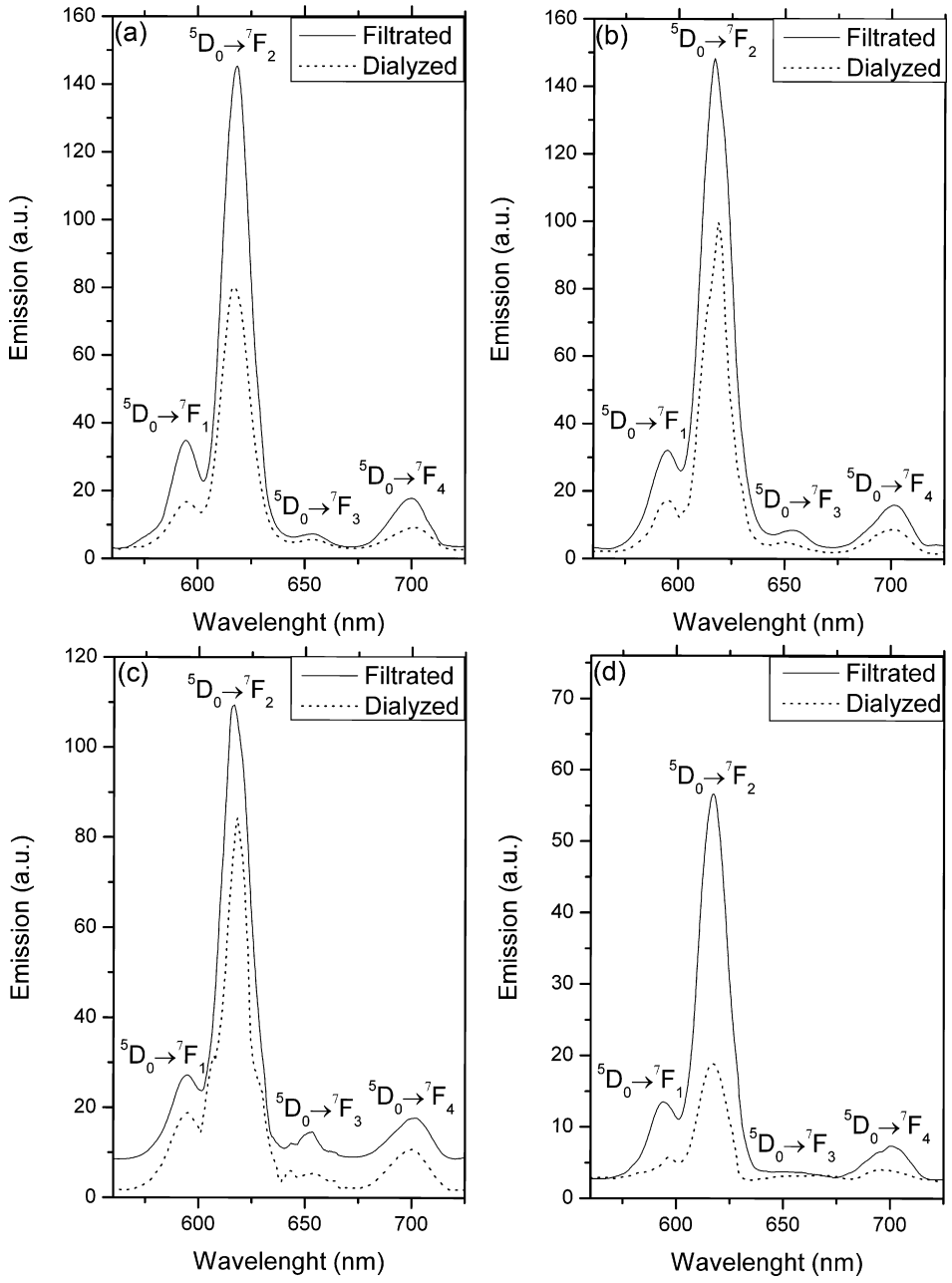

Fig. 6. PL spectra of filtrated and dialyzed samples of Eu^{3+} doped TiO_2 nanocrystals (a) and prolate nanospheroids synthesized with different concentrations of nanotubes in precursor dispersions: 25 mg/10 mL (b), 50 mg/10 mL (c) and 75 mg/10 mL (d).

TiO_2 prolate nanospheroids is less than in the nanoparticles ($d < 20$ nm) due to bigger dimensions and lower curvature [23]. Such assertion is further supported by the observed higher overall decrease in the concentration of Eu^{3+} ions in the nanocrystals after dialysis (0.24 at.% Eu^{3+}) compared with the dialyzed prolate nanospheroids (0.42 at.% Eu^{3+}).

Emission spectra of the filtrated and dialyzed Eu^{3+} doped TiO_2 prolate nanospheroids synthesized using titania nanotubes as a precursor in concentrations 50 mg/10 mL and 75 mg/10 mL are shown in Fig. 6c and d, respectively. All the peaks characteristic of the $^5D_0 \rightarrow {}^7F_1$, $^5D_0 \rightarrow {}^7F_2$, $^5D_0 \rightarrow {}^7F_3$ and $^5D_0 \rightarrow {}^7F_4$ transitions were observed in PL spectra (Fig. 6c and d). The peak intensity ratios between the dialyzed and filtrated samples were preserved as in the doped prolate nanospheroids (Fig. 6b), with the highest amount of dopant ions (Table 1). A large decrease in the intensity of $^5D_0 \rightarrow {}^7F_2$ transition in the dialyzed sample (0.041 at.% Eu^{3+}) when compared with filtrated (0.2 at.% Eu^{3+}) sample (Fig. 6d) is an indication of the initially larger amount of Eu^{3+} ions positioned in low symmetry sites that can be removed by dialysis.

The general characteristic of the Eu^{3+} doped TiO_2 nanocrystals and nanospheroids synthesized in this way is a much stronger electric dipole transition compared with magnetic dipole transition. Such behavior indicates that the Eu^{3+} ions mainly take low symmetry sites without an inversion center in the host anatase TiO_2 lattice.

Table 1
The R values and concentrations of Eu^{3+} ions in filtrated and dialyzed samples of Eu^{3+} doped TiO_2 nanoparticles and prolate nanospheroids (Sample 1, Sample 2, and Sample 3) synthesized using precursor dispersions with different concentrations of nanotubes and same concentration of Eu^{3+} ions (6.4×10^{-4} M).

	$C_{filtrated}$ (at.% Eu^{3+})	$C_{dialyzed}$ (at.% Eu^{3+})	$R_{filtrated}$	$R_{dialyzed}$
Nanoparticles (25 mg/10 mL)	0.7	0.24	4.18	4.8
Sample 1 (25 mg/10 mL)	0.5	0.42	4.62	4.77
Sample 2 (50 mg/10 mL)	0.34	0.18	4.03	4.52
Sample 3 (75 mg/10 mL)	0.2	0.041	4.19	3.36

An insight into the degree of disorder around the Eu^{3+} cation and the breaking of centro-symmetry can be obtained from the intensities ratio, R, of the $^5D_0 \rightarrow {}^7F_2$ and $^5D_0 \rightarrow {}^7F_1$ transitions, the so called asymmetric ratio [32]. A higher degree of disorder around Eu^{3+} cations and lower symmetry are indicated by higher value of R. Also, an increase in R of $^5D_0 \rightarrow {}^7F_2$ and $^5D_0 \rightarrow {}^7F_1$ transitions implies the strengthening of the covalency of Eu–O bond (reduction of Eu–O bond distance) [33]. The R values, along with the concentrations of Eu^{3+} ions in the filtrated and dialyzed samples of Eu^{3+} doped TiO_2 nanocrystals and prolate nanospheroids, are presented in Table 1. The doped nanocrystals and the prolate nanospheroids, Sample 1, were synthesized using the same concentrations of nanotubes precursor dispersion (25 mg/10 mL) and Eu^{3+} ions (6.4×10^{-4} M).

According to our measurements, the R values in the dialyzed samples of Eu^{3+} doped TiO_2 nanocrystals and nanospheroids (Samples 1 and 2) are higher than the R values of the corresponding filtrated (Table 1). Only for the nanospheroids, Sample 3, is the R value of the filtrated samples higher than that of the dialyzed (Table 1). The values of R about 4 in all investigated samples of Eu^{3+} doped TiO_2 nanocrystals and prolate nanospheroids (Table 1) are in agreement with their crystal structure and the possible presence of OH groups on the nanoparticle surface.

In our filtrated samples of Eu^{3+} doped TiO_2 nanocrystals and the prolate nanospheroids, the dopant ions are simultaneously distributed on the surface and in the interior of the particles. Recently, Dossot et al. have obtained the value of R close to 4 for the partially hydroxylated Eu^{3+} ions with Eu–OH bonds in Eu^{3+} doped glass sample [29]. Almost the same value of R was reported by Tachikawa et al. for Eu^{3+} doped TiO_2 nanoparticles in a poly(vinyl alcohol); after modification of the nanoparticle surface with octadecyltrimetoxysilane, the shift of R to higher value was observed [32]. The observed lower values of R for the filtrated than for the dialyzed samples could be due to the presence of two different kinds of OH groups (15 OH^-/nm^2) and physisorbed water molecules on the particle surface that affect the photoluminescence property of Eu^{3+} ions on the surface [34,35].

The residual Eu^{3+} ions in the interior region of dialyzed TiO_2 nanocrystals and prolate nanospheroids in ambient air can cause higher R values [32]. The higher R value can be explained by the creation of oxygen vacancies and lattice distortions after substitution of Eu^{3+} for Ti^{4+} ions in the TiO_2 host. Also, in the dialyzed samples of nanocrystals and Samples 1 and 2, the existence of Eu^{3+}–O^{2-}–Ti^{4+} bonds and the fact that Ti^{4+} has larger radius and lower electronegativity than O^{2-} induced the increase of the degree of covalence of Eu–O bond [33]. Values of R close to 4, according to Grausem et al. [29], indicate that the centro-symmetry is broken; however, degree of the disorder is not as important as in the case of the amorphous phase of Eu^{3+} doped glass sample, where $R = 7.69$ was reported.

4. Conclusion

In summary, Eu^{3+} doped faceted titania nanocrystals and prolate nanospheroids were synthesized by a two step hydrothermal method. The presence of Eu^{3+} ions did not affect the formation of faceted titania nanocrystals and nanospheroids using titania nanotubes as a precursor. The resulting Eu^{3+} doped TiO_2 nanocrystals and the prolate nanospheroids belong to the anatase polymorph. The nanopowders exhibited red photoluminescence by direct excitation of Eu^{3+} ions. The increase of R value after dialysis indicates the increased of contributions of the dopant in the interior region of dialyzed samples (nanocrystals, Samples 1 and 2) with lower site symmetry to the emission and also increasing of the covalency of Eu–O bond. This study demonstrates the possible route to the preparation of rare earth element doped faceted titania nanocrystals and prolate nanospheroids using nanotubes as precursor.

Acknowledgments

The financial support for this work was provided by the Ministry of Education and Science of Republic of Serbia (projects 172056 and 45020). The authors are grateful to Prof. Phil Ahrenkiel from South Dakota School of Mines & Technology, USA for TEM measurements of titania nanotubes.

References

[1] D.K. Williams, B. Bihari, B.M. Tissue, J.M. McHale, Preparation and fluorescence spectroscopy of bulk monoclinic Eu^{3+}:Y_2O_3 and comparison to Eu^{3+}:Y_2O_3 nanocrystals, Journal of Physical Chemistry B 102 (1998) 916–920.
[2] K. Riwotzki, M. Haase, Wet-chemical synthesis of doped colloidal nanoparticles: YVO_4:Ln (Ln = Eu Sm, Dy), Journal of Physical Chemistry B 102 (1998) 10129–10135.
[3] A.A. Bol, R. van Beek, A. Meijerink, On the incorporation of trivalent tare earth ions in II–VI semiconductor nanocrystals, Chemistry of Materials 14 (2002) 1121–1126.
[4] A.V. Firth, D.J. Cole-Hamilton, J.W. Allen, Optical properties of CdSe nanocrystals in a polymer matrix, Applied Physics Letters 75 (1999) 3120–3123.

[5] G. Blasse, B.C. Grabmaier, Luminescent Materials, Springer-Verlag, Berlin, Germany, 1994.
[6] J.G. Li, X. Wang, K. Watanabe, T. Ishigaki, Phase structure and luminescence properties of Eu^{3+}-doped TiO_2 nanocrystals synthesized by Ar/O_2 radio frequency thermal plasma oxidation of liquid precursor mists, Journal of Physical Chemistry B 110 (2006) 1121–1127.
[7] Q. Xiao, Y. Liu, L. Liu, R. Li, W. Luo, X. Chen, Eu^{3+}-doped In_2O_3 nanophosphors: electronic structure and optical characterization, Journal of Physical Chemistry C 114 (2010) 9314–9321.
[8] M. Ikeda, J.G. Li, N. Kobayashi, Y. Moriyoshi, H. Hamanaka, T. Ishigaki, Phase formation and luminescence properties in Eu^{3+}-doped TiO_2 nanoparticles prepared by thermal plasma pyrolysis of aqueous solutions, Thin Solid Films 516 (2008) 6640–6644.
[9] E. Zaleta-Alejandre, M. Zapata-Torres, M. Garcia-Hipolito, M. Aguilar-Frutis, G. Alarcon-Flores, J. Guzman-Mendoza, C. Falcon, Structural and luminescent properties of europium doped TiO_2 thick films synthesized by the ultrasonic spray pyrolysis technique, Journal of Physics D: Applied Physics 42 (2009) 095102.
[10] X. Chen, W. Luo, Optical spectroscopy of rare earth ion-doped TiO_2 nanophosphors, Journal of Nanoscience and Nanotechnology 10 (2010) 1482–1494.
[11] T. Kasuga, M. Hiramatsu, A. Hoson, T. Sekino, K. Niihara, Titania nanotubes prepared by chemical processing, Advanced Materials 11 (1999) 1307–1311.
[12] Z.V. Šaponjić, N.M. Dimitrijević, D.M. Tiede, A.J. Goshe, X. Zuo, L.X. Chen, A.S. Barnard, P. Zapol, L. Curtiss, T. Rajh, Shaping nanometer-scale architecture through surface chemistry, Advanced Materials 17 (2005) 965–971.
[13] Z.V. Šaponjić, N.M. Dimitrijević, O.G. Poluektov, L.X. Chen, E. Wasinger, U. Welp, D.M. Tiede, X. Zuo, T. Rajh, Charge separation and surface reconstruction: a Mn^{2+} doping study, Journal of Physical Chemistry B 110 (2006) 25441–25450.
[14] N.M. Dimitrijević, Z.V. Šaponjić, B.M. Rabatic, O.G. Poluektov, T. Rajh, Effect of size and shape of nanocrystalline TiO_2 on photogenerated Charges. An EPR Study, Journal of Physical Chemistry C 111 (2007) 14597–14601.
[15] R.D. Shannon, Revised effective ionic radii and systematic studies of interatomic distances in halides and chalcogenides, Acta Crystallographica Section A 32 (1976) 751–767.
[16] Q.G. Zheng, Z.J. Ding, Z.M. Zhang, Synthesis, structure and optical properties of Eu^{3+}/TiO_2 nanocrystals at room temperature, Journal of Luminescence 118 (2006) 301–307.
[17] H. Tang, H. Berger, P.E. Schmid, F. Lévy, G. Burri, Photoluminescence in TiO_2 anatase single crystals, Solid State Communications 87 (1993) 847–850.
[18] http://www.webelements.com/titanium/atom_sizes.html.
[19] W. Luo, R. Li, X. Chen, Host-sensitized luminescence of Nd^{3+} and Sm^{3+} ions incorporated in anatase titania nanocrystals, Journal of Physical Chemistry C 113 (2009) 8772–8777.
[20] L. Diamandescua, F. Vasiliu, D. Tarabasanu-Mihaila, M. Federa, A.M. Vlaicu, C.M. Teodorescu, D. Macovei, I. Enculescu, V. Parvulescu, E. Vasile, Structural and photocatalytic properties of iron- and europium-doped TiO_2 nanoparticles obtained under hydrothermal conditions, Materials Chemistry and Physics 112 (2008) 146–153.
[21] T. Sekia, K. Ichimura, M. Igarashi, S. Kurita, Absorption spectra of anatase TiO_2 single crystals heat-treated under oxygen atmosphere, Journal of Physics and Chemistry of Solids 61 (2000) 1237–1242.
[22] W. Luo, R. Li, G. Liu, M.R. Antonio, X. Chen, Evidence of trivalent europium incorporated in anatase TiO_2 nanocrystals with multiple sites, Journal of Physical Chemistry C 112 (2008) 10370–10377.
[23] B.M. Rabatic, N.M. Dimitrijevic, R.E. Cook, Z.V. Saponjic, T. Rajh, Spatially confined corner defects induce chemical functionality of TiO_2 nanorods, Advanced Materials 18 (2006) 1033–1037.
[24] V.S. Marques, L.S. Cavalcante, J.C. Sczancoski, E.C. Paris, J.M.C. Teixeira, J.A. Varela, F.S. De Vicente, M.R. Joya, P.S. Pizani, M. Siu Li, M.R.M.C. Santos, E. Longo, Synthesis of $(Ca,Nd)TiO_3$ powders by complex polymerization, rietveld refinement and optical properties, Spectrochimica Acta, Part A 74 (2009) 1050–1059.
[25] A. Bahtat, M.C.M. DeLucas, B. Jacquier, B. Varrel, M. Bouazaoui, J. Mugnier, IR luminescence decays and radiative lifetime of the ^{4}Isol132 level in Er^{3+} doped sol–gel TiO_2 planar waveguide, Optical Materials 7 (1997) 173–179.
[26] Z. Lu, J. Wang, Y. Tang, Y. Lia, Synthesis and photoluminescence of Eu^{3+}-doped $Y_2Sn_2O_7$ nanocrystals, Journal of Solid State Chemistry 177 (2004) 3075–3079.
[27] L. Chen, T. Rajh, W. Jäger, J. Nedeljković, M.C. Thurnauer, X-ray absorption reveals surface structure of titanium dioxide nanoparticles, Journal of Synchrotron Radiation 6 (1999) 445–447.
[28] T. Rajh, L.X. Chen, K. Lukas, T. Liu, M.C. Thurnauer, D.M. Tiede, Surface restructuring of nanoparticles: an efficient route for ligand–metal oxide crosstalk, Journal of Physical Chemistry B 106 (2002) 10543–10552.
[29] J. Grausem, M. Dossot, S. Cremel, B. Humbert, F. Viala, P. Mauchien, Local heterogeneity for a Eu^{3+}-doped glass evidenced by time-resolved fluorescence spectroscopy coupled to scanning near-field optical microscopy, Journal of Physical Chemistry B 110 (2006) 11259–11266.
[30] P.H. Butler, Point Group Symmetry Application: Method and Tables, Plenum, New York, 1981.
[31] Y. Liu, W. Luo, H. Zhu, X. Chen, Optical spectroscopy of lanthanides doped in wide band-gap semiconductor nanocrystals, Journal of Luminescence 131 (2011) 415–422.
[32] T. Tachikawa, T. Ishigaki, J.G. Li, M. Fujitsuka, T. Majima, Defect-mediated photoluminescence dynamics of Eu^{3+} doped TiO_2 nanocrystals revealed at the single-particle or single-aggregate level, Angewandte Chemie (International Edition) 47 (2008) 5348–5352.
[33] Z. Zhao, Q.G. Zeng, Z.M. Zhang, Z.J. Ding, Optical properties of Eu^{3+}-doped TiO_2 nanocrystalline under high pressure, Journal of Luminescence 122–123 (2007) 862–865.
[34] P. Ghosh, A. Patra, Influence of surface coating on physical properties of TiO_2/Eu^{3+} nanocrystals, Journal of Physical Chemistry C 111 (2007) 7004–7010.
[35] A. Cordoba, J. Luque, Mechanism of surface dehydration of anatase ($Ti0_2$), Physical Review B 31 (1985) 8111–8118.